Cell Reports

Article

Leucine-sensing mechanism of leucyl-tRNA synthetase 1 for mTORC1 activation

Graphical abstract

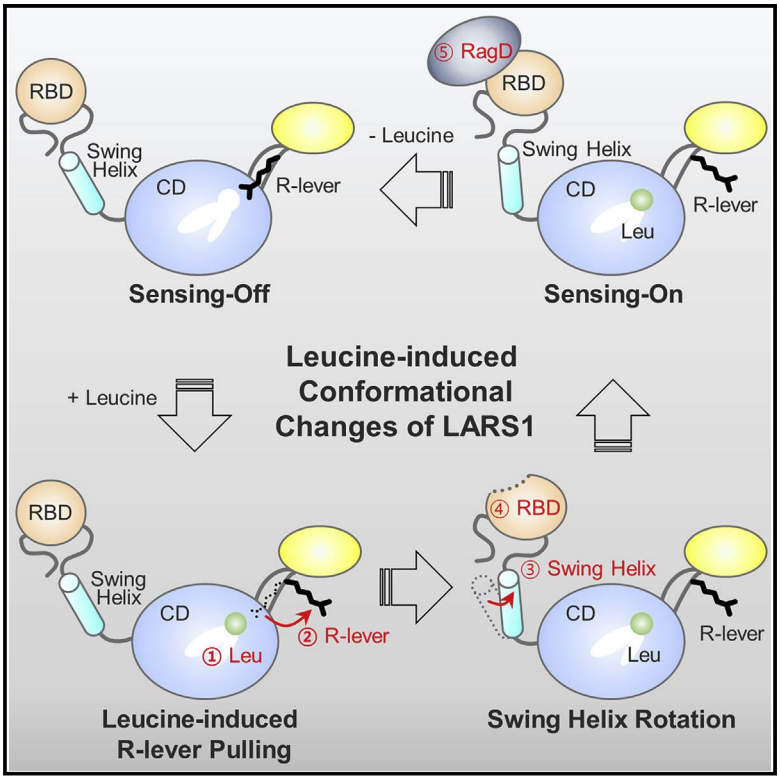

Highlights

- Leucine binding induces conformational change of LARS1 for RagD binding
- ATP increases leucine binding to LARS1 for enhanced RagD binding
- Leucine-controlled R-lever triggers long-range conformational change of LARS1
- LARS1 cycles between "sensing on (leucine+)" and "sensing off (leucine−)" states.

Authors

Sulhee Kim, Ina Yoon, Jonghyeon Son, ..., Jung Min Han, Kwang Yeon Hwang, Sunghoon Kim

Correspondence

chahong@korea.ac.kr (K.Y.H.), sunghoonkim@yonsei.ac.kr (S.K.)

In brief

Kim et al. report leucine-induced conformational changes in LARS1 to control the mTORC1 pathway. The results mechanistically validate LARS1 as an amino acid sensor and provide insight into how amino acid and ATP levels are sensed together via LARS1.

Kim et al., 2021, Cell Reports *35*, 109031
April 27, 2021
https://doi.org/10.1016/j.celrep.2021.109031

CellPress

Cell Reports

CellPress
OPEN ACCESS

Article

Leucine-sensing mechanism of leucyl-tRNA synthetase 1 for mTORC1 activation

Sulhee Kim,[1,7] Ina Yoon,[2,7] Jonghyeon Son,[1,7] Junga Park,[1] Kibum Kim,[3,4] Ji-Ho Lee,[1] Sam-Yong Park,[5] Beom Sik Kang,[6] Jung Min Han,[3,4] Kwang Yeon Hwang,[1,*] and Sunghoon Kim[2,8,*]

[1]Department of Biotechnology, College of Life Sciences and Biotechnology, Korea University, Seoul 02841, Republic of Korea
[2]Medicinal Bioconvergence Research Center, Institute for Artificial Intelligence and Biomedical Research, College of Pharmacy & College of Medicine, Gangnam Severance Hospital, Yonsei University, Incheon 21983, Republic of Korea
[3]Yonsei Institute of Pharmaceutical Sciences, College of Pharmacy, Yonsei University, Incheon 21983, Republic of Korea
[4]Interdisciplinary Program of Integrated OMICS for Biomedical Science, Graduate School, Yonsei University, Seoul 03722, Republic of Korea
[5]Drug Design Laboratory, Graduate School of Medical Life Science, Yokohama City University, Yokohama 230-0045, Japan
[6]School of Life Science and Biotechnology, KNU Creative BioResearch Group, Kyungpook National University, Daegu 41566, Republic of Korea
[7]These authors contributed equally
[8]Lead contact
*Correspondence: chahong@korea.ac.kr (K.Y.H.), sunghoonkim@yonsei.ac.kr (S.K.)
https://doi.org/10.1016/j.celrep.2021.109031

SUMMARY

Leucyl-tRNA synthetase 1 (LARS1) mediates activation of leucine-dependent mechanistic target of rapamycin complex 1 (mTORC1) as well as ligation of leucine to its cognate tRNAs, yet its mechanism of leucine sensing is poorly understood. Here we describe leucine binding-induced conformational changes of LARS1. We determine different crystal structures of LARS1 complexed with leucine, ATP, and a reaction intermediate analog, leucyl-sulfamoyl-adenylate (Leu-AMS), and find two distinct functional states of LARS1 for mTORC1 activation. Upon leucine binding to the synthetic site, H251 and R517 in the connective polypeptide and ^{50}FPYPY^{54} in the catalytic domain change the hydrogen bond network, leading to conformational change in the C-terminal domain, correlating with RagD association. Leucine binding to LARS1 is increased in the presence of ATP, further augmenting leucine-dependent interaction of LARS1 and RagD. Thus, this work unveils the structural basis for leucine-dependent long-range communication between the catalytic and RagD-binding domains of LARS1 for mTORC1 activation.

INTRODUCTION

Mechanistic target of rapamycin complex 1 (mTORC1) controls anabolic cell growth and proliferation by coupling growth factors, amino acids, oxygen, and energy status with cellular responses such as lipid synthesis, nucleotide synthesis, protein synthesis, and autophagy (Dibble and Manning, 2013; Kim and Guan, 2019; Saxton and Sabatini, 2017), and the pathological relevance of dysregulated mTORC1 signaling pathway is reported in various diseases, including cancer, epilepsy, and aging (Iyer et al., 2012; Johnson et al., 2013; Sun et al., 2013; Wagle et al., 2014).

Amino acids activate mTORC1 through Rag guanosine triphosphatase (GTPase) heterodimers composed of RagA or RagB bound to RagC or RagD (Sancak et al., 2008). The activity of Rag GTPases is determined by their states of guanine nucleotide bound, guanosine diphosphate (GDP) or guanosine triphosphate (GTP), which is regulated by guanine nucleotide exchange factors (GEFs) and GTPase-activating proteins (GAPs) (Bar-Peled et al., 2012, 2013; Han et al., 2012; Shen and Sabatini, 2018; Tsun et al., 2013). Among the four possible configurations, only heterodimers of GTP-loaded RagA or RagB and GDP-loaded RagC or RagD activate mTORC1. Among 20 amino acids, leucine, glutamine, and arginine are known to be potent activators of the mTORC1 pathway (Jewell et al., 2015; Kim et al., 2002; Nicklin et al., 2009; Wang et al., 2015), and specific sensors for some amino acids (leucine, arginine, and S-adenosylmethionine) are identified along with their downstream routes for mTORC1 stimulation (Chantranupong et al., 2016; Gu et al., 2017; Han et al., 2012; Wolfson et al., 2016). In addition, studies on three-dimensional (3D) structures of amino acid sensors such as Sestrin2, cellular arginine sensor for mTORC1 (CASTOR), and solute carrier 38, family A member 9 (SLC38A9) in complex with their corresponding amino acids revealed an amino acid-sensing mechanism (Lei et al., 2018; Saxton et al., 2016a, 2016b).

Leucyl-tRNA synthetase 1 (LARS1) is one of the class I aminoacyl-tRNA synthetases (ARSs) consisting of multi-tRNA synthetase complex (MSC) along with several different tRNA

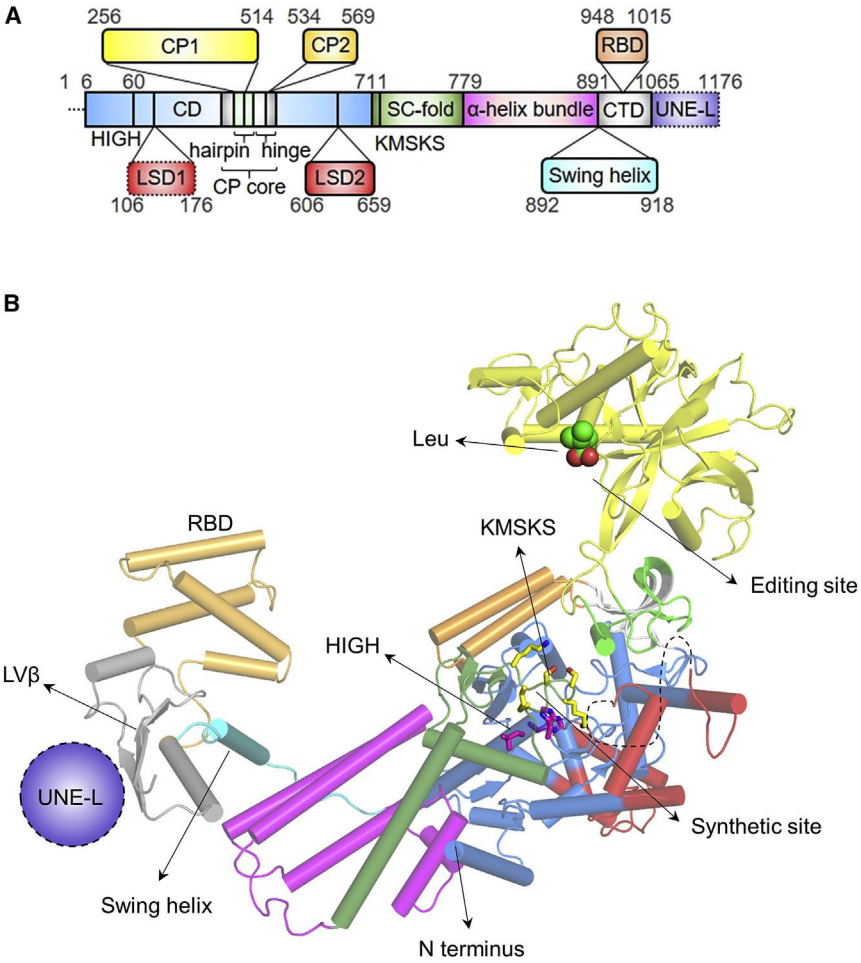

Figure 1. Overall structure of LARS1

(A) Domain arrangement of LARS1. CD, catalytic domain; LSD, leucine-specific domain; CP, connective polypeptide; SC, stem-contact; CTD, C-terminal domain; RBD, RagD-binding domain; UNE-L, unnamed domain of LARS1.

(B) Cartoon representation of LARS1^{methyl}-Leu-AMS^{syn}. Leucine in the editing site (Leu^{CP1}) is designated as a green sphere model. Synthetic site would contain each of leucine, Leu-AMS, and ATP, respectively. Functional domains of LARS1 are represented with different colors, as described in (A). Swing helix, LVβ, and RBD of LARS1 CTD are colored cyan, gray, and orange, respectively. KMSKS motif and HIGH region are represented by yellow and magenta stick models, respectively. Disordered regions are designated as dashed lines. Disordered UNE-L domain is represented as purple circle.

synthetases (Eriani et al., 1990; Fukunaga and Yokoyama, 2005a; Ribas de Pouplana and Schimmel, 2001). LARS1 first activates leucine through the adenosine triphosphate (ATP)-dependent formation of Leu-AMP and then transfers leucine to the cognate tRNAs to form Leu-tRNA^{Leu}, which is used in translation at ribosome (Ibba and Soll, 2000; Kim et al., 2011; Kwon et al., 2019). Although LARS1 works as an enzyme for protein synthesis, it also serves as one of the leucine sensors to activate the mTORC1 pathway in human as well as yeast (Bonfils et al., 2012; Han et al., 2012; Kim et al., 2016, 2017; Lee et al., 2018; Son et al., 2019; Yoon et al., 2016). In the presence of leucine, LARS1 is translocated to the lysosome and facilitates the conversion of RagD-GTP to RagD-GDP form, resulting in mTORC1 activation.

Although LARS1 is reported as a leucine sensor for mTORC1 signaling, it is still not well understood how leucine binding can trigger its RagD-binding capability. Although several studies have revealed crystal structures of LARS in bacteria and archaea (Cusack et al., 2000; Fukunaga and Yokoyama, 2005a, 2005b; Palencia et al., 2012), the residues crucial for RagD binding are absent or not conserved in those species (Han et al., 2012), making it difficult to give insight into leucine-sensing mechanism of LARS1. As for human LARS1, a recent study revealed crystal structures of C-terminal 106 amino acid-truncated LARS1 in complex with leucyl-sulfamoyl-adenylate (Leu-AMS) and 2′-(L-norvalyl)amino-2′-deoxyadenosine (Nva2AA) (PDB: 6LPF) or with Leu-AMS and AN6426-AMP (PDB: 6LR6) (Liu et al., 2020), suggesting some structural basis for interaction with RagD. However, given that Leu-AMS analogs inhibit leucine-induced stimulation of the mTORC1 pathway (Yoon et al., 2017, 2019), what kind of conformational change of LARS1 occurs in complex with leucine still remains unclear.

To understand amino acid sensing mechanism, here we investigated the conformational changes of LARS1 upon binding to leucine, ATP, and the analog of reaction intermediate Leu-AMP, Leu-AMS, and how this mechanism could affect RagD association and mTORC1 activation.

RESULTS

Specific binding of LARS1 with leucine

To examine the specific binding of leucine to LARS1, we incubated LARS1 and EPRS1 (glutamyl-prolyl-tRNA synthetase 1), another component of MSC, with isotope-labeled leucine and observed specific leucine binding to LARS1 but not to EPRS1 (Figure S1A). The incubation of LARS1 with leucine, but not with other branched-chain amino acids (isoleucine and valine) or tryptophan, increased the inflection temperature as shown by the T_i value (Figure S1B), also supporting specific binding of leucine to LARS1.

Overall structure of LARS1

We obtained different crystal structures of LARS1 (1–1,176 aa), complexed with leucine, ATP, and Leu-AMS at resolutions of 3.30, 3.15, and 3.15 Å, respectively (Figures 1A and 1B). One

molecule of LARS1 is located in the asymmetric unit (ASU) with ~73% of solvent. It contains three main domains including the catalytic domain (CD), editing (connective polypeptide [CP1]), and C-terminal domain (CTD). The CTD of LARS1 is connected to the main body through a 35-Å-long α-helix ("swing helix") and is further divided into the RagD-binding domain (RBD) and long variable arm motif including three β-strands (LVβ). The disordered UNE-L domain attached to the C-terminal of LARS1 (1,066–1,176 aa) interacts with other MSC components (Freedman et al., 1985; Ling et al., 2005; Rossmann et al., 1974). The overall fold of LARS1 CD (6–230 and 537–707 aa) is similar to that of archaeal LARS (*Pyrococcus horikoshii*; *Ph*LARS, PDB: 1WKB; Fukunaga and Yokoyama, 2005b; 4–174 and 511–641 aa) with a root-mean-square deviation (RMSD) of 1.4 Å. The CD is composed of a Rossmann fold of eight α helices and five β strands that contains HIGH and KMSKS motifs that recognize ATP (Freedman et al., 1985; Rossmann et al., 1974). The SC (stem-contact)-fold domain contains a common structural feature, β-α-α-β-α fold. The α-helix bundle domain, followed by CTD, consists of five α helices. The characteristic features of archaeal/eukaryotic LARS are also found in human LARS1. Leucine-specific domain 1 (LSD1: 106–176 aa), which is located between α3 and α4 of the CD, is fully disordered, and LSD2 (606–659 aa) shows a similar helix-turn-helix fold to *Ph*LARS (Yan et al., 2013). CP1 is inserted within the CP1 hairpin motif, and CP2, which consists of two α helices, is inserted within the CP core motif, where it functions as a hinge. The overall differences between LARS1-Leu^{syn} (PDB: 6KQY) (996 Cα atoms) and LARS1-ATP^{syn} (PDB: 6KID) (1,001 Cα atoms), LARS1-Leu^{syn} and LARS1-Leu-AMS^{syn} (PDB: 6KIE) (933 Cα atoms), and LARS1-ATP^{syn} and LARS1-Leu-AMS^{syn} are shown with RMSDs of 1.5, 1.3, and 1.1 Å, respectively. Although the CD and CP1 show similar structures between LARS1-Leu^{syn} and LARS1-Leu-AMS^{syn} (RMSD ~ 1.1 Å), the orientation of LARS1-Leu^{syn} CTD including RBD is different from the other structures (LARS1-Leu-AMS^{syn} and LARS1-ATP^{syn}). Detailed information about structure determination is shown in Table S1.

Structure of LARS1 in complex with leucine

LARS1 complexed with leucine (LARS1-Leu^{syn}; PDB: 6KQY) contains leucine in the editing site (Leu^{CP1}) and the synthetic site (Leu^{syn}) of the CD at a resolution of 3.30 Å (Figure 2A). Leu^{syn} protrudes toward the catalytic core. Y52, Y54, H91, H251, L677, and H681 form a cavity allowing hydrophobic interactions with leucine. P53 and Y54 also form hydrogen bonds with the carboxyl and amine groups of leucine (Figure 2B). Leu^{syn}-binding residues are evolutionarily conserved (Figure S1C), suggesting the significance of the residues involved in leucine binding. Eliminating the hydrophobic interaction cavity by substituting alanine for Y52, Y54, and H91 (Y52A/Y54A, H91A, and Y52A/Y54A/H91A) abolished LARS1 leucine binding, as determined by isotope-labeled leucine binding assay and microscale thermophoresis (MST) (Figures 2C and S1D). Co-immunoprecipitation of LARS1 with RagD revealed that leucine-dependent interaction of the two proteins was decreased in these leucine binding-deficient mutants, leading to the decreased conversion of RagD-GTP to RagD-GDP form and leucine-dependent phosphorylation of ribosomal protein S6 kinase (S6K), a substrate of mTOR kinase, while the levels of ARF1-GTP form and S6K were not changed irrespective of leucine stimulation (Figures 2D and 2E). Thus, leucine binding to the LARS1 synthetic site is crucial for leucine sensing, leading to mTORC1 activation.

Effect of ATP binding on leucine sensing of LARS1

Next, we investigated the role of ATP, another substrate of LARS1, on leucine binding and mTORC1 activation in accordance with LARS1 catalytic activity, as the previous study suggested the possible need of ATP for leucine binding to LARS1 (Yoon et al., 2020). As expected, leucine binding to LARS1 was increased in the presence of ATP, as monitored by isotope-labeled leucine binding assay, isothermal titration calorimetry (ITC), and MST (Figures 3A–3C). Consistently, the interaction of LARS1 and RagD was increased in an ATPαS-dependent manner only in the presence of leucine (Figure 3D), implying that the binding of ATP to LARS1 helps leucine-induced activation of mTORC1.

Although we could not obtain crystals of LARS1 containing both leucine and ATPαS (a surrogate of ATP) in the synthetic site, we obtained a crystal structure of LARS1 harboring ATP in the synthetic site (ATP^{syn}) and leucine in the editing site (Leu^{CP1}) (LARS1-ATP^{syn}; PDB: 6KID) (Figure 4A). The phosphate moiety of ATP is oriented toward ^{716}KMSKS^{720} motif, opposite to the catalytic core, and the β and γ phosphates of ATP form hydrogen bonds with H251 and E257, respectively. The NH_2 moiety of the ATP adenine ring, which is bound to histidine pockets (H60, H63, and H709), protrudes toward the ^{716}KMSKS^{720} motif with a distance about 3.4 Å, and the hydroxyl group of the sugar ring interacts with S673 and D676 (Figure 4B). LARS1 mutants with alanine substitution at residues important for ATP binding (H60A/H63A, E257A, and S673A/D676A) showed decreased capability of leucine binding as well as ATP binding, as measured using isotope-labeled leucine binding assay and MST (Figures 4C, S2A, and S2B), further supporting the significance of ATP binding in leucine binding. In contrast to LARS1 wild-type (WT), the ATP binding-defective mutants did not exhibit leucine-dependent mTORC1 activation on the basis of co-immunoprecipitation with RagD, GTP-agarose pull-down assay, and the phosphorylation patterns of S6K in response to leucine (Figures 4D and 4E).

LARS1 structures of sensing-on and sensing-off states for mTORC1 activation

After binding with leucine and ATP, LARS1 synthesizes Leu-AMP from leucine through the hydrolysis of ATP to adenosine monophosphate (AMP) and pyrophosphate (PPi) (Kim et al., 2011). Leu-AMS, an analog of reaction intermediate Leu-AMP and also known as a catalytic inhibitor of LARS1 (Lee et al., 2018), disrupted leucine binding to LARS1 (Figure S3A). When monitoring the effect of Leu-AMS on the mTORC1 pathway, cells incubated with Leu-AMS showed decreased mTORC1 stimulation in response to leucine (Figure S3B). Therefore, we regarded Leu-AMS-bound LARS1 as an inactive conformation for mTORC1 stimulation and obtained the third LARS1 structure (LARS1-Leu-AMS^{syn}; PDB: 6KIE) complexed with Leu-AMS in the synthetic site (Leu-AMS^{syn}) and leucine in the editing site (Leu^{CP1}) (Figure S3C) to compare the structural difference

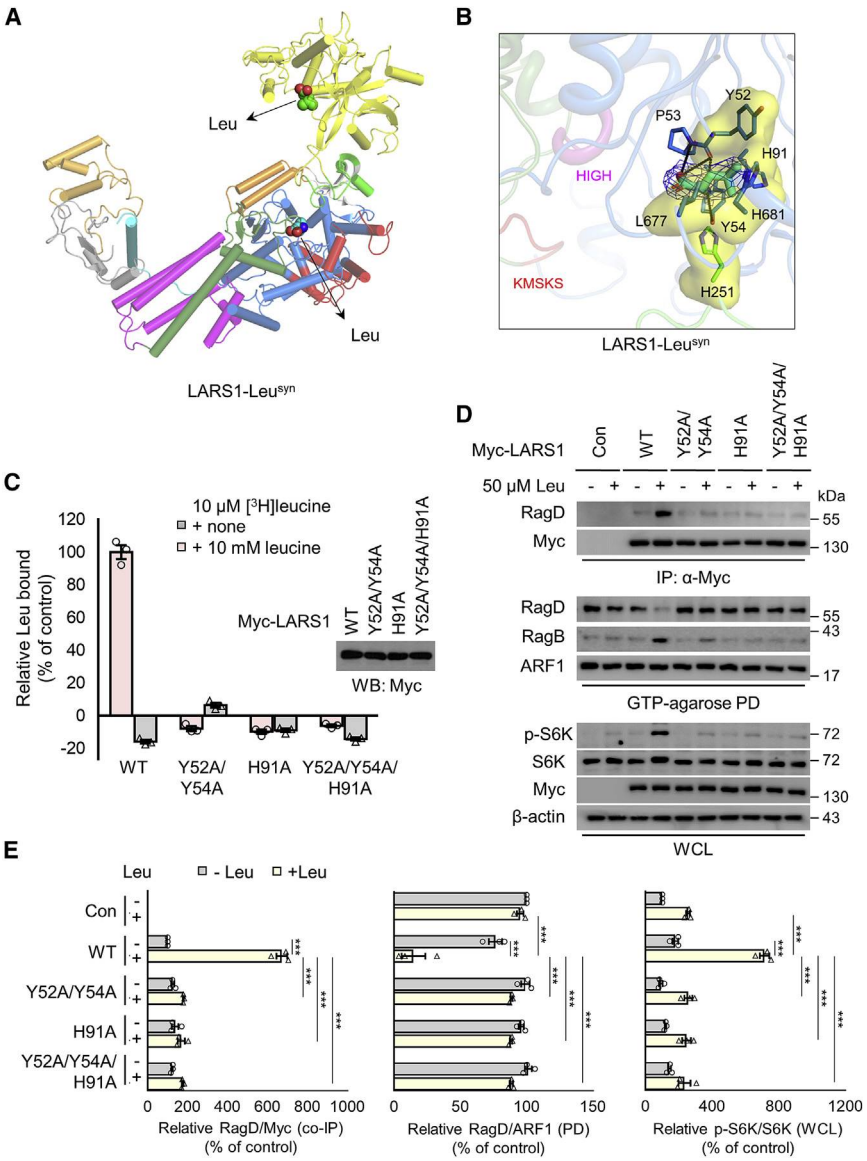

Figure 2. Functional effect of leucine binding to LARS1 for mTORC1 activation

(A) Overall structure of LARS1 complexed with leucine in the synthetic site (Leu^{syn}) and the editing site (Leu^{CP1}). Leu^{syn} and Leu^{CP1} are designated as cyan and green sphere models, respectively.

(B) Zoomed view of the synthetic site in the LARS1-Leu^{syn} structure. Residues involved in the hydrophobic interaction with leucine are yellow surface model. The hydrogen bonds between LARS1 and leucine are shown as black dotted lines. Leucine is shown as a cyan stick model, and the 2Fo-Fc map of leucine is represented as a blue mesh model at a 2.0 sigma contour level. HIGH and KMSKS motifs are magenta and red, respectively.

(C) Myc-LARS1 wild-type (WT) and the indicated mutants expressed in HEK293T cells were immunoprecipitated with anti-Myc antibody and incubated with [^{3}H]leucine in the presence or absence of unlabeled leucine. Binding of [^{3}H]leucine to LARS1 was determined using liquid scintillating counter (LSC) (n = 3; mean ± SEM). Unlabeled leucine was used to monitor the specific binding of [^{3}H]leucine.

(D and E) HEK293T cells expressing LARS1 WT and the indicated mutants were starved of leucine and then stimulated with leucine. Leucine-dependent activities of LARS1 to the mTORC1 pathway were determined by the co-precipitation of RagD with LARS1 (upper), the conversion of RagD-GTP to RagD-GDP form with the reverse conversion of RagB-GDP to RagB-GTP form (middle), and S6K phosphorylation patterns (lower) (D). Immunoblot images are representative of three biological replicates. The band intensity of immunoblot images was quantified using Multi Gauge (E) (n = 3; mean ± SEM). Empty vector transfection is used as negative control (Con) for Myc-LARS1 overexpression. ARF1 was used as a negative control for leucine-dependent -GTP and -GDP state changes. β-actin was used as protein loading control. IP, immunoprecipitation; PD, pull-down; WCL, whole-cell lysates. ***$p < 0.001$, two-way ANOVA.

between the "sensing-on" and "sensing-off" states for mTORC1 activation. The leucine moiety of Leu-AMS protrudes to the catalytic core, and the adenine ring, hydroxyl group of the sugar ring, and sulfamoyl group interact with L710, S66, S673, and H63 (Figure S3D).

The sensing-off (LARS1-Leu-AMS^{syn}, sensing-off$^{Leu\text{-}AMS}$) and sensing-on (LARS1-Leu^{syn}, sensing-on^{+}) structures unveiled the difference in orientation of CTD to CD. The CTD swing helix of LARS1-Leu^{syn} rotates inward ~25° compared with that of LARS1-Leu-AMS^{syn} (Figures 5A and 5B). This leucine binding-induced conformation change in detail was examined by comparing the structures of LARS1-Leu^{syn} and LARS1-Leu-AMS^{syn} (Figures 5C–5F). In LARS1-Leu^{syn}, leucine occupation in the synthetic site forms a hydrogen bond between H251 and Y54, changing the orientation of the CP1 hairpin motif relative to LARS1-Leu-AMS^{syn} (Figure 5E). The R517 residue of LARS1-Leu-AMS^{syn} forms hydrogen bonds with H251 and N56 in the CD (Figure 5C). In contrast, LARS1-Leu^{syn}'s R517 protrudes in the opposite direction of the synthetic site and interacts with D244 in the CP1 hairpin motif in sensing-on^{+} (Figures 5E, 5F, and S3E). LARS1-Leu-AMS^{syn} alters the surrounding hydrogen-bonding network such that R517 can be flipped inward to the synthetic site and connects to the network (Figure 5C). As a result, D244, S516, and S241 form a more rigid hydrogen-bonding network in the sensing-off$^{Leu\text{-}AMS}$ conformation that is reinforced by hydrogen bonds between G245, Q246, and T576 (Figures 5D and S3F). Together, R517 works as leucine-dependent lever ("R-lever") to induce local alteration of hydrogen-bonding network between the CP1 hairpin motif and CD and eventually CTD rotation.

To validate the significance of the LARS1 conformational change for activating the mTORC1 pathway, we prepared the

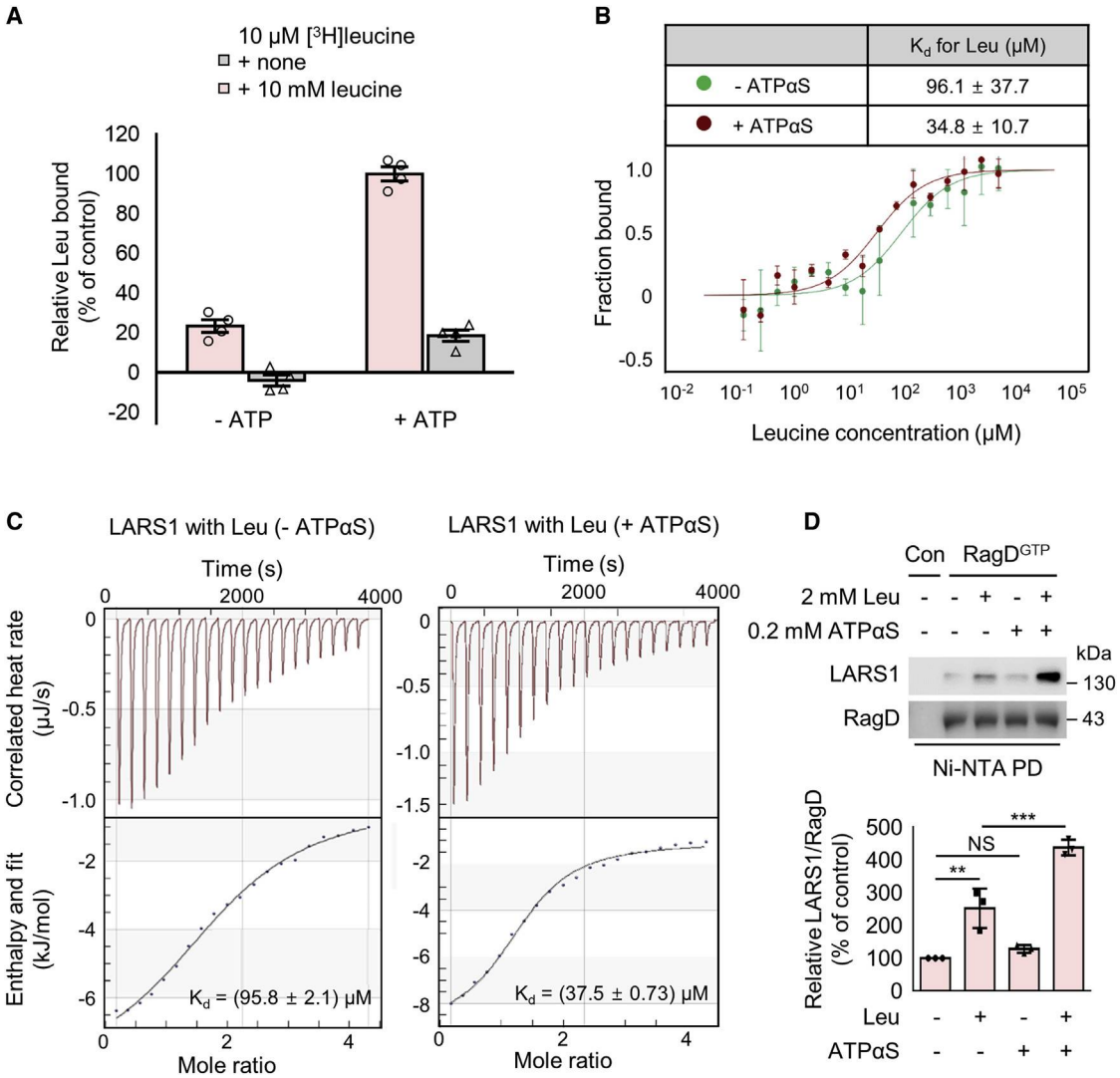

Figure 3. Functional significance of ATP for leucine binding to LARS1

(A) Myc-LARS1 expressed in HEK293T cells was immunoprecipitated with anti-Myc antibody and incubated with [^{3}H]leucine in the presence or absence of ATP. The binding of [^{3}H]leucine to LARS1 was determined using LSC (n = 4; mean ± SEM).

(B) Binding affinities of leucine to LARS1 in the presence or absence of ATP analog, ATPαS, were determined using MST experiments. The exact K_d values are listed in the table (n = 3; mean ± SD).

(C) The K_d values of leucine to LARS1 in the presence or absence of 1 mM ATPαS were determined using isothermal titration calorimetry (ITC).

(D) The effect of leucine and ATPαS on the interaction of LARS1 and RagD^{GTP}. LARS1 in HEK293T cell lysates was co-precipitated with His-RagD^{GTP} (Q121L) immobilized to Ni-NTA beads under the indicated conditions. Immunoblot images are representative of three biological replicates (n = 3; **p < 0.01 and ***p < 0.001, one-way ANOVA; mean ± SEM). NS, not significant.

alanine substitution mutants at the residues H251 and R517, which are involved in conformational change (H251A, R517A, and H251A/R517A), and then evaluated the activity for leucine-induced mTORC1 stimulation. The interaction of LARS1 and RagD was decreased in these mutants, which led to an increase in the amount of RagD-GTP form and a decrease in the phosphorylation of S6K (Figures 5G and 5H), suggesting that leucine-induced conformational change of the R-lever and CP1 hairpin motif contributes to mTORC1 activation.

Then, we compared all three LARS1 structures complexed with leucine, ATP, and Leu-AMS around the ^{50}FPYPY^{54}, CP1 hairpin motif, and R-lever region (Figures 5I–5K). Superimposition of the structures revealed that LARS1-Leu^{syn} shows sensing-on state, while LARS1-ATP^{syn} and LARS1-Leu-AMS^{syn} show sensing-off state on the basis of the orientation of R-lever (Figure 5L).

We further validated our sensing-on and sensing-off structures by comparing structural features with PDB: 6LPF (Liu et al., 2020). Superimposition of both structures on the basis of the CD revealed that overall structure of 6LPF is similar to our structures, showing RMSDs of 1.1–3.1 Å (Figure S4). Consistent with our model of swing helix rotation, 6LPF shows a similar

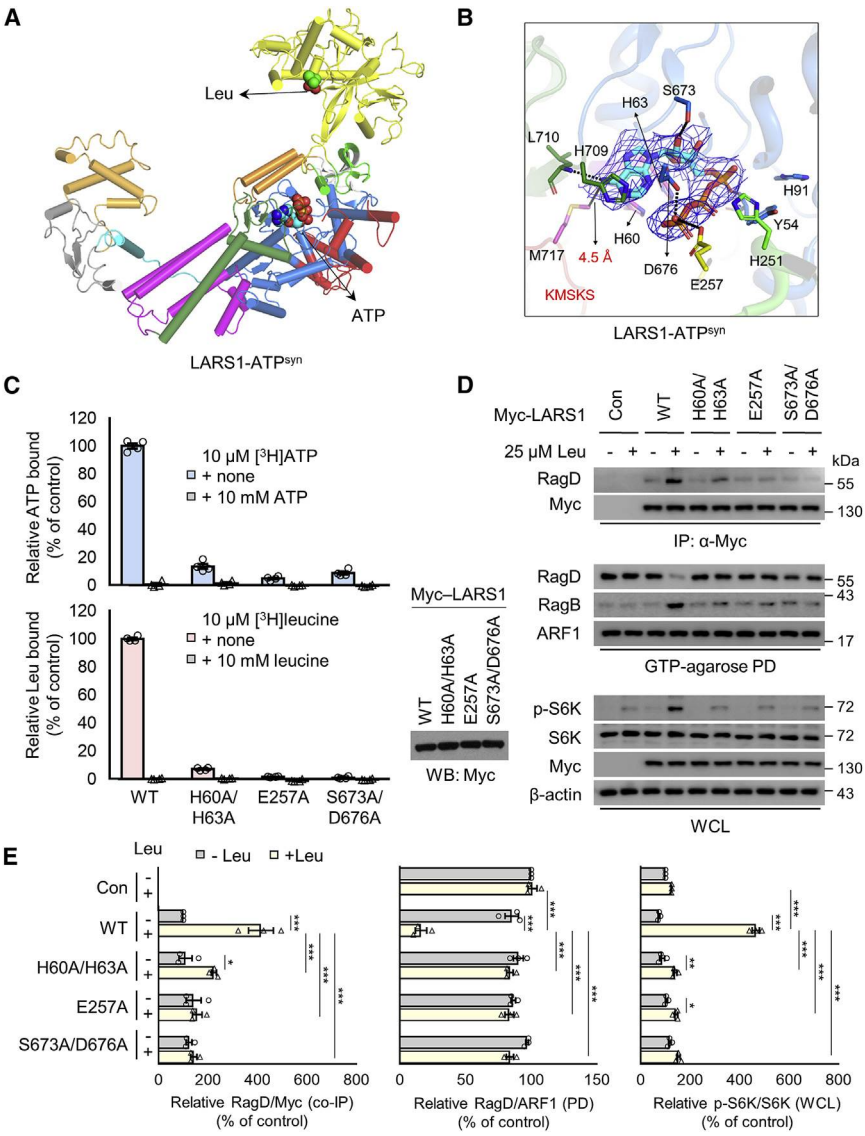

Figure 4. Effect of ATP binding on the leucine binding to LARS1 and mTORC1 activation

(A) Overall structure of LARS1 complexed with ATP at the synthetic site (ATP^{syn}) and in the editing site (Leu^{CP1}). ATP^{syn} and Leu^{CP1} are designated as cyan and green sphere models, respectively.

(B) Zoomed view of the synthetic site of the LARS1-ATP^{syn} structure. ATP is shown as a cyan stick model, and the 2Fo-Fc map of ATP is represented as a blue mesh model at a 2.0 sigma contour level. KMSKS motif is red. The distance between the NH_2 moiety of adenine ring and side chain of M717 in KMSKS motif is denoted by a black line. The hydrogen bonds between LARS1 and ATP are shown as black dotted lines.

(C) Myc-LARS1 WT or the indicated mutants expressed in HEK293T cells were immunoprecipitated with anti-Myc antibody and incubated with [^{3}H]ATP or [^{3}H]leucine. The binding of [^{3}H]ATP (upper) or [^{3}H]leucine (lower) to LARS1 WT and mutants were determined using LSC (n = 4; mean ± SEM).

(D and E) HEK293T cells expressing Myc-LARS1 WT and mutants were starved of leucine and then stimulated with leucine. Leucine-dependent interaction with RagD (upper), conversion of RagD-GTP to RagD-GDP (middle), and S6K phosphorylation patterns (lower) were determined as above (D). Immunoblot images are representative of three biological replicates. The band intensity of immunoblot images was quantified using Multi Gauge (E) (n = 3; mean ± SEM). *p < 0.05, **p < 0.01, and ***p < 0.001, two-way ANOVA.

location of swing helix to sensing-off structures (LARS1-Leu-AMS^{syn}, LARS1-ATP^{syn}, and LARS1^{methyl}-Leu-AMS^{syn}) (Figures S4B–S4D), whereas the swing helix of 6LPF is rotated about 23° compared with that of sensing-on structures (LARS1-Leu^{syn}) (Figure S4A). These results suggested that LARS1 in complex with Leu-AMS in the synthetic site shows the sensing-off functional state irrespective of different crystal conditions, including the complexed molecules in the editing site. In addition, LARS1-Leu^{syn} shows a unique conformational change of the CTD compared with 6LPF.

The effect of swing helix rotation on mTORC1 activation

To further examine the significance of the R-lever to swing helix movement for LARS1 binding to RagD, we monitored the alteration of overall tertiary structure in the presence or absence of leucine and ATPαS in LARS1 WT and mutants. In addition to LARS1 R517A, we also prepared N802C/G889C and A888P/G889P mutants. N802 is located in the CD, and A888 and G889 are located in the connecting loop between the swing helix and CD (Figures 6A–6C). Both of the mutants are expected to disturb the swing helix movement because N802C/G889C would possibly increase the interaction between the CD and the connecting loop, and two consecutive prolines in A888P/G889P would confer rigidity to the connecting loop (Figures 6B and 6C). These mutants showed similar binding affinity to leucine compared with LARS1 WT (Figure S5A). LARS1 WT and mutants showed similar composition of the secondary structures independently of the absence or presence of leucine and ATPαS (Figure S5B) as determined by far-ultraviolet (UV) circular dichroism. However, near-UV circular dichroism spectra suggested a difference in their tertiary structures (Figure 6D). Although LARS1 N802C/G889C and A888P/G889P showed different near-UV circular dichroism spectra from R517A in the absence of leucine and ATPαS (Figure 6D, left), LARS1 N802C/G889C, A888P/G889P, and R517 showed similar near-UV circular dichroism spectra in the presence of leucine and ATPαS, implying that ablation of the R-lever disturbs the swing helix rotation (Figure 6D, right).

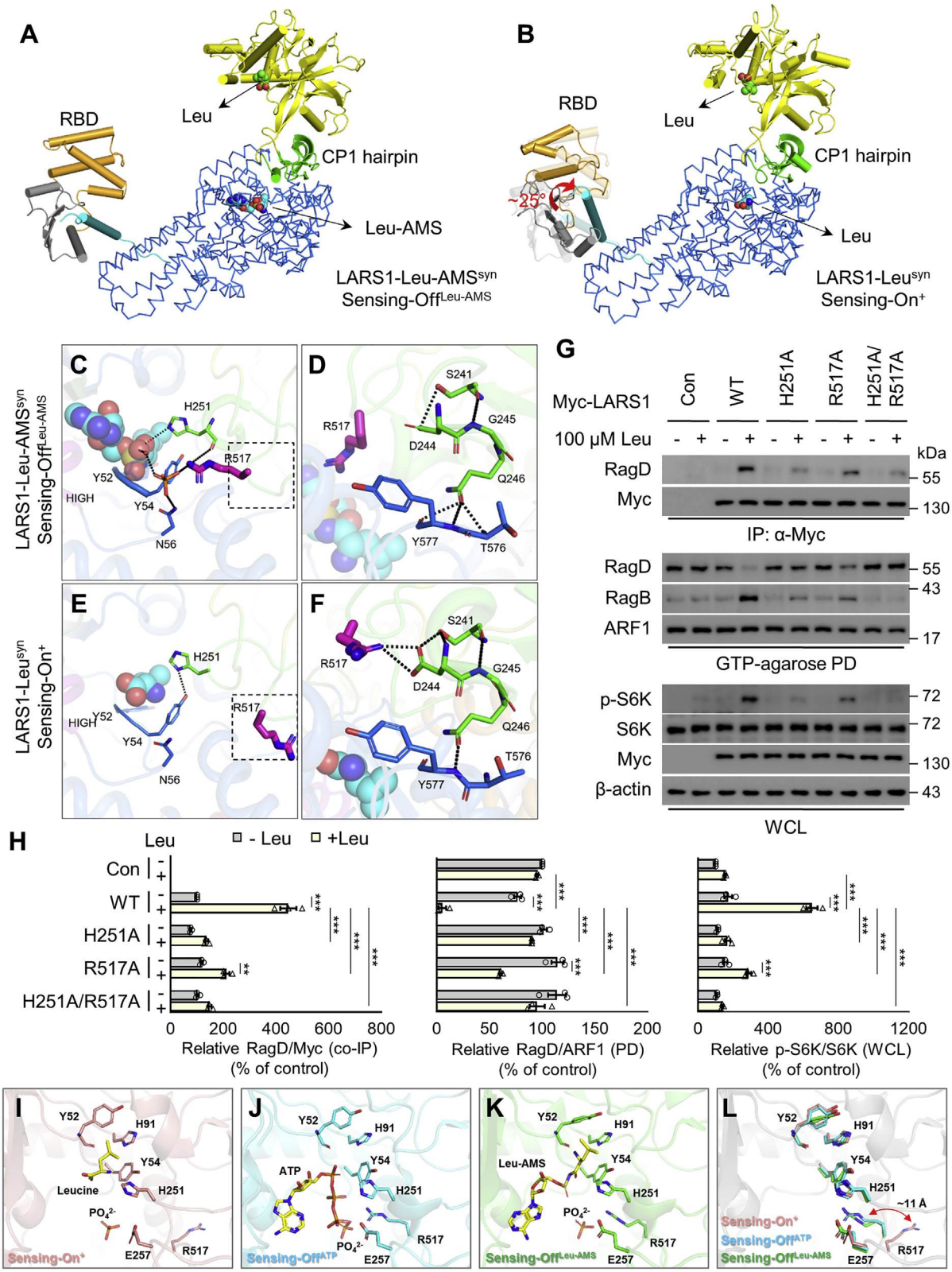

(legend on next page)